nature physics

LETTERS

PUBLISHED ONLINE: 24 JANUARY 2010 | DOI: 10.1038/NPHYS1515

Observation of parity–time symmetry in optics

Christian E. Rüter[1], Konstantinos G. Makris[2], Ramy El-Ganainy[2], Demetrios N. Christodoulides[2], Mordechai Segev[3] and Detlef Kip[1]*

One of the fundamental axioms of quantum mechanics is associated with the Hermiticity of physical observables[1]. In the case of the Hamiltonian operator, this requirement not only implies real eigenenergies but also guarantees probability conservation. Interestingly, a wide class of non-Hermitian Hamiltonians can still show entirely real spectra. Among these are Hamiltonians respecting parity–time (*PT*) symmetry[2–7]. Even though the Hermiticity of quantum observables was never in doubt, such concepts have motivated discussions on several fronts in physics, including quantum field theories[8], non-Hermitian Anderson models[9] and open quantum systems[10,11], to mention a few. Although the impact of *PT* symmetry in these fields is still debated, it has been recently realized that optics can provide a fertile ground where *PT*-related notions can be implemented and experimentally investigated[12–15]. In this letter we report the first observation of the behaviour of a *PT* optical coupled system that judiciously involves a complex index potential. We observe both spontaneous *PT* symmetry breaking and power oscillations violating left–right symmetry. Our results may pave the way towards a new class of *PT*-synthetic materials with intriguing and unexpected properties that rely on non-reciprocal light propagation and tailored transverse energy flow.

Before we introduce the concept of spacetime reflection in optics, we first briefly outline some of the basic aspects of this symmetry within the context of quantum mechanics. In general, a Hamiltonian $\hat{H} = \hat{p}^2/2m + V(\hat{x})$ (where $\hat{x}$ and $\hat{p}$ are position and momentum operators respectively, m is mass and V is the potential) is considered to be PT symmetric, $PT\hat{H} = \hat{H}PT$, provided that it shares common eigenfunctions with the PT operator[1,16–21]. This condition corresponds to an exact or unbroken PT symmetry, as opposed to that of broken PT symmetry, where, even though $PT\hat{H} = \hat{H}PT$ is still valid, $\hat{H}$ and PT (or any other antilinear operator) possess different eigenvectors[22]. For the case considered here, given that the action of the parity P and time T operators is defined as $\hat{p} \to -\hat{p}, \hat{x} \to -\hat{x}$ and $\hat{p} \to -\hat{p}, \hat{x} \to \hat{x}, i \to -i$, respectively, it then follows that a necessary (but not sufficient) condition for a Hamiltonian to be PT symmetric is $V(\hat{x}) = V^*(-\hat{x})$. In other words, PT symmetry requires that the real part of the potential V is an even function of position x, whereas the imaginary part is odd; that is, the Hamiltonian must have the form $\hat{H} = \hat{p}^2/2m + V_R(\hat{x}) + i\varepsilon V_I(\hat{x})$, where $V_{R,I}$ are the symmetric and antisymmetric components of V, respectively[12–14]. Clearly, if $\varepsilon = 0$, this Hamiltonian is Hermitian. It turns out that, even if the antisymmetric imaginary component is finite, this class of potentials can still allow for both bound and radiation states, all with entirely real spectra. This is possible as long as ε is below some threshold, $\varepsilon < \varepsilon_{th}$. If, on the other hand, this limit is crossed ($\varepsilon > \varepsilon_{th}$), the spectrum ceases to be real and starts to involve imaginary eigenvalues. This signifies the onset of a spontaneous PT symmetry-breaking, that is, a 'phase transition' from the exact to broken-PT phase[7,20].

In optics, several physical processes are known to obey equations that are formally equivalent to that of Schrödinger in quantum mechanics. Spatial diffraction and temporal dispersion are perhaps the most prominent examples. In this work we focus our attention on the spatial domain, for example optical beam propagation in PT-symmetric complex potentials. In fact, such PT 'optical potentials' can be realized through a judicious inclusion of index guiding and gain/loss regions[7,12–14]. Given that the complex refractive-index distribution $n(x) = n_R(x) + in_I(x)$ plays the role of an optical potential, we can then design a PT-symmetric system by satisfying the conditions $n_R(x) = n_R(-x)$ and $n_I(x) = -n_I(-x)$.

In other words, the refractive-index profile must be an even function of position x whereas the gain/loss distribution should be odd. Under these conditions, the electric-field envelope E of the optical beam is governed by the paraxial equation of diffraction[13]:

$$i\frac{\partial E}{\partial z} + \frac{1}{2k}\frac{\partial^2 E}{\partial x^2} + k_0[n_R(x) + in_I(x)]E = 0$$

where $k_0 = 2\pi/\lambda$, $k = k_0 n_0$, λ is the wavelength of light in vacuum and n_0 represents the substrate index.

Ultimately, it will be of interest to synthesize artificial periodic optical systems showing unusual features stemming from PT symmetry[13,14]. Yet, it is first imperative to understand PT behaviour at a single-cell level. In integrated optics, such a single PT element can be realized in the form of a coupled system[7,12], with only one of the two parallel channels being optically pumped to provide gain γ_G for the guided light, whereas the neighbour arm experiences loss γ_L (Fig. 1a). Under these conditions and by using the coupled-mode approach, the optical-field dynamics in the two coupled waveguides are described by

$$i\frac{dE_1}{dz} - i\frac{\gamma_{Geff}}{2}E_1 + \kappa E_2 = 0, \qquad i\frac{dE_2}{dz} + i\frac{\gamma_L}{2}E_2 + \kappa E_1 = 0 \qquad (1)$$

where $E_{1,2}$ represent field amplitudes in channels 1 and 2, $\kappa = \pi/(2L_c)$ is the coupling constant with coupling length L_c and the effective gain coefficient is $\gamma_{Geff} = \gamma_G - \gamma_L$. From previous considerations, PT symmetry demands that $\gamma_{Geff} = \gamma_L = \gamma$. The behaviour of this non-Hermitian system can be explained by considering the structure of its eigenvectors, above and below the phase-transition point $\gamma/(2\kappa) = 1$. Below this threshold the supermodes are given by $|1,2\rangle = (1, \pm\exp(\pm i\theta))$, with corresponding eigenvalues being $\pm\cos\theta$, where $\sin\theta = \gamma/2\kappa$. At phase transition (the 'exceptional

[1]Clausthal University of Technology, Institute of Energy Research & Physical Technologies, Leibnizstr. 4, 38678 Clausthal-Zellerfeld, Germany, [2]University of Central Florida, School of Optics-CREOL, Orlando, Florida 32816-2700, USA, [3]Technion-Israel Institute of Technology, Department of Physics, 32000 Haifa, Israel. *e-mail: kip@hsu-hh.de.

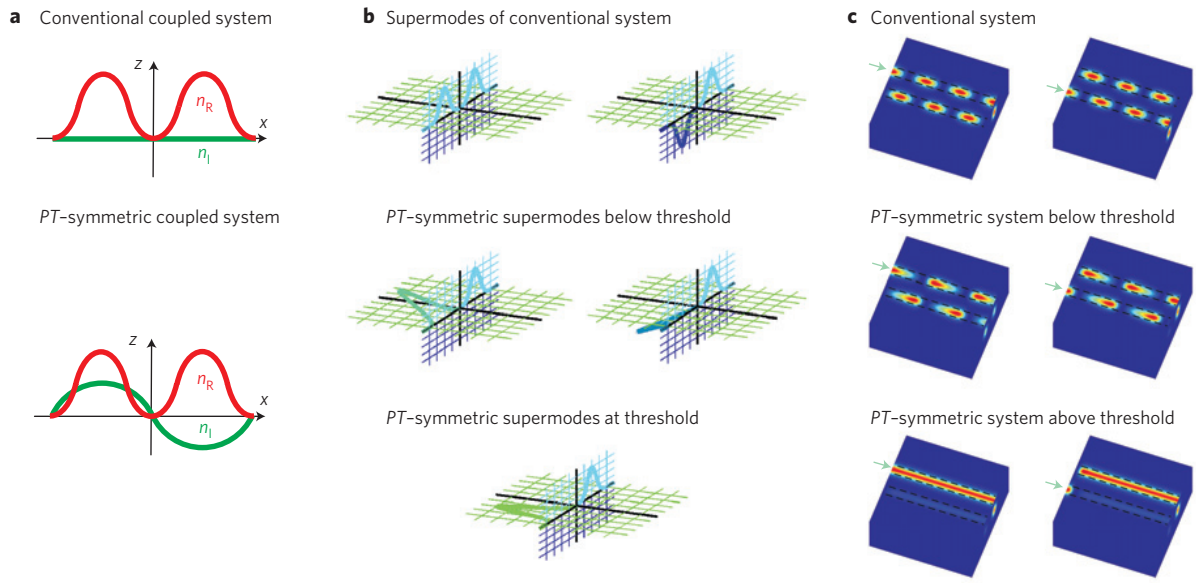

Figure 1 | Conventional and *PT*-symmetric coupled optical systems. a, Real (n_R, red line) and imaginary (n_I, green line) parts of the complex refractive-index distribution. **b**, Supermodes of a conventional system, and of a *PT*-symmetric arrangement below and above threshold. **c**, Optical wave propagation when the system is excited at either channel 1 or channel 2. For the conventional case, wave propagation is known to be reciprocal, whereas in a *PT*-symmetric system light propagates in a non-reciprocal manner both below and above threshold.

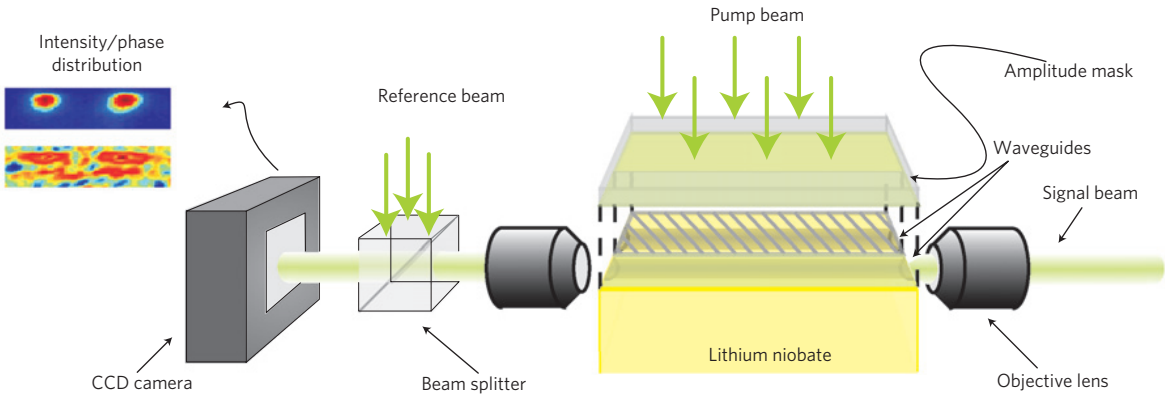

Figure 2 | Experimental set-up. An Ar^+ laser beam (wavelength 514.5 nm) is coupled into the arms of the structure fabricated on a photorefractive $LiNbO_3$ substrate. An amplitude mask blocks the pump beam from entering channel 2, thus enabling two-wave mixing gain only in channel 1. A CCD camera is used to monitor both the intensity and phases at the output.

point'), the modes coalesce to $|1,2\rangle = (1,i)$, where the amplitudes in the two channels have the same magnitude[23,24]. Above threshold, that is, for $\gamma > 2\kappa$, $|1,2\rangle = (1, i\exp(\mp\theta))$, where in this range $\cosh\theta = \gamma/2\kappa$ and the two eigenvalues are $\mp i\sinh\theta$. We emphasize that, unlike Hermitian systems, these eigenmodes are no longer orthogonal. Instead, the basis is now skewed. This in turn has important implications for optical-beam dynamics including a non-reciprocal response and power oscillations. For a conventional Hermitian system ($\gamma = 0$), any superposition of the two (symmetric and antisymmetric, see Fig. 1b) eigenmodes leads to reciprocal wave propagation: obviously, the light distribution in Fig. 1c (top) obeys left–right symmetry. This situation changes when the coupled system involves a gain/loss dipole. If the gain increases but is still below threshold, the relative phase differences ϑ between the two field components increase from their initial values at 0 and π, respectively, and finally, at threshold, the two modes coalesce at $\vartheta = \pi/2$ (see Fig. 1b). More interestingly, light propagation is now obviously non-reciprocal: by exchanging the input channel from 1 to 2 in Fig. 1c (middle) we obtain an entirely different output state. This behaviour is altered drastically above threshold (Fig. 1c, bottom). In this regime light always leaves the sample from channel 1, irrespective of the input—again in a non-reciprocal fashion. This can be explained by noting that, above threshold, the system's eigenvalues are complex, with the corresponding amplitudes either exponentially increasing or decaying. Thus only one supermode effectively survives. Here it is worth noting that any coupled system with an asymmetric gain–loss profile can be mathematically transformed into a *PT*-symmetric one. In particular, this is true for an asymmetric loss/loss-type potential (coupled states with low/high losses), showing a 'passive' *PT* system[25]. Very recently, for such a system, loss-induced optical transparency was experimentally demonstrated.

Here we observe non-reciprocal wave propagation in an 'active' *PT*-symmetric coupled waveguide system based on Fe-doped $LiNbO_3$. As such, this structure shows richer dynamics and enables us to explore a wider range of behaviour not previously accessible because of fixed losses. We use Ti in-diffusion to form the symmetric index profile $n_R(x)$. Optical gain γ_G (the typical magnitude is a few cm^{-1} in Fe-doped $LiNbO_3$) is provided through two-wave mixing using the material's photorefractive

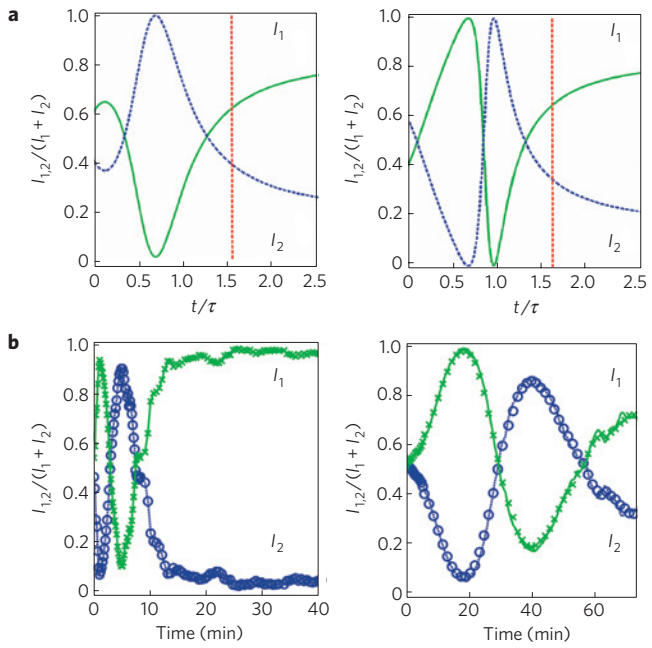

Figure 3 | Computed and experimentally measured response of a *PT*-symmetric coupled system. a, Numerical solution of the coupled equations (1) describing the *PT*-symmetric system. The left (right) panel shows the situation when light is coupled into channel 1 (2). Red dashed lines mark the symmetry-breaking threshold. Above threshold, light is predominantly guided in channel 1 experiencing gain, and the intensity of channels 1 and 2 depends solely on the magnitude of the gain. **b**, Experimentally measured (normalized) intensities at the output facet during the gain build-up as a function of time.

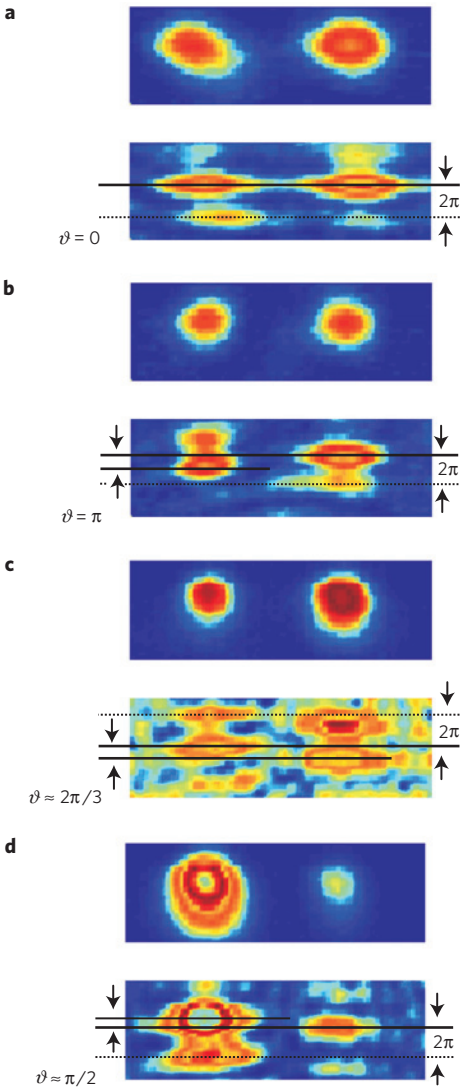

Figure 4 | *PT* supermode phase measurements. a–d, Intensity distribution (upper panels) and phase relation (lower panels) of conventional (**a**,**b**) and *PT*-symmetric (**c**,**d**) systems. **a**,**b**, Measured relative phases of an even (**a**) and odd (**b**) eigenstate associated with a conventional system. **c**,**d**, Phase relation corresponding to a *PT*-symmetric system below (**c**) and above (**d**) threshold. Although below threshold (**c**) the phase difference lies in the interval $[0,\pi]$, depending on the magnitude of gain, above threshold this value is fixed at $\pi/2$, as shown in **d**.

nonlinearity[26,27]. A mask on top of the sample is used to partially block the pump light, to provide amplification in only one channel (see the experimental set-up in Fig. 2). Both the output intensity and the phase relation between the two channels (using interference with a plane reference wave) are monitored by a CCD (charge-coupled device) camera. In our system, losses arise from the optical excitation of electrons from Fe^{2+} centres to the conduction band. On the other hand, the optical two-wave mixing gain (which is proportional to the concentration of Fe^{3+} centres) has a finite response time[26]. Assuming an exponential temporal build-up, $\gamma_G(t) = \gamma_{max}[1 - \exp(-t/\tau)]$ with Maxwell time constant τ, the evolution of the intensity distribution at the output facet can be monitored as a function of time t. In other words, the state of the system below, at and above threshold can be directly observed at different instants t (refs 7, 13).

Although equations (1) can be solved analytically, we here obtain the output intensities $I_1 \sim |E_1|^2$, $I_2 \sim |E_2|^2$ as a function of gain $\gamma_G(t)$ by numerical integration. Figure 3a shows results of two such simulations when $\gamma_L = 2\kappa$, $\gamma_{max} = 2.5\gamma_L$, where channel 1 (Fig. 3a, left-hand side) or channel 2 (Fig. 3a, right-hand side) has been excited. At $t = 0$ the system starts from $\gamma_G = 0$ and shows a reciprocal response. However, as the gain builds up at $t > 0$ and the *PT* structure is tuned below threshold (which is reached for $t/\tau \approx 1.6$), wave propagation becomes strongly non-reciprocal (with different numbers of zero-crossings, depending on the ratio L/L_c; see Fig. 3a). At the threshold the two supermodes become degenerate; however, the intensities of the two fields are slightly different. The reason lies in the limited length L of our sample: at threshold, the pure coalesced eigenstate $|1,2\rangle = (1, i)$ of our system (excited by an input state (1, 0) or (0, 1), respectively) is approached adiabatically only for infinitely long propagation, $L/L_c \to \infty$. Above threshold the output of the *PT* system is no longer sensitive to the input conditions. In this regime, one supermode is exponentially amplified whereas the other decays.

The experimental response of this $LiNbO_3$ *PT*-symmetric optical system (with $\kappa = 1.9\,cm^{-1}$ and $L = 2\,cm$) is shown in Fig. 3b. In all our experiments we used low input power levels (signal power $\sim 25\,nW$ and pump intensity $I_p = 0.5\,mW\,cm^{-2}$ when exciting channel 2, and twice these values when exciting channel 1) to avoid any index perturbations (including the situation above threshold, where intensity increases rapidly), which may in turn spoil the symmetry in $n_R(x)$ (refs 28, 29). Figure 3b (left-hand side and right-hand side) depicts the temporal behaviour of the output intensity distribution when channel 1 and 2 is excited, respectively. We note that the build-up time constants τ in these two situations are different owing to different intensities used during excitation. As a result, the threshold is reached faster ($t_{th,1} \approx 10$ min) in the first case as compared with the latter ($t_{th,2} \approx 70$ min). By taking this into

account, we find an excellent agreement between our experiments and numerical simulations.

Another manifestation of *PT* symmetry is the relative phase difference ϑ between the two elements of the same eigenmode—which can be measured at the output facet of the sample. These results are depicted in Fig. 4. For $\gamma_G = 0$, the phases corresponding to the even and odd supermodes are $\vartheta = 0$ and $\vartheta = \pi$, respectively, as in conventional arrangements (Fig. 4a,b). When the gain is further increased and the system is below threshold, the two eigenstates are not orthogonal and their phases can be anywhere (depending on $\gamma/2\kappa$) in the interval $[0, \pi]$. An example is given in Fig. 4c, where a phase difference of $\vartheta \approx 2\pi/3$ was estimated from our measurements. Finally, Fig. 4d illustrates the situation slightly above the exceptional point. In this case the phase is fixed at $\vartheta = \pi/2$, irrespective of $\gamma/2\kappa$, again in good agreement with theoretical predictions.

Our results can be easily extended to transversely periodic media, enabling new intriguing effects such as *PT* solitons, double-refraction or synthetic systems with tailored transverse flow of optical energy, and thus pave the way for developing new non-reciprocal optical components, where light is propagating forward and backward in a different fashion. This letter has made the simplest demonstration of *PT* effects: just a coupled two-channel system. However, the vision is to incorporate nonlinearities and construct sophisticated *PT* systems, such as *PT* optical lattices, *PT*-based solitons and so on. Last but not least, the phase-transition or exceptional point has been intriguing researchers for a long time, because the eigenmodes associated with that point are self-orthogonal, and as such their amplitudes should diverge[7]. In addition, in optical *PT* lattices, anomalous transport or discrete diffraction can occur in the neighbourhoods of such points, as indicated in ref. 13. Is this self-orthogonality a physical property with truly unique and experimentally observable quantities? This and related questions are now within experimental reach.

Received 3 August 2009; accepted 17 December 2009; published online 24 January 2010

References

1. Shankar, R. *Principles of Quantum Mechanics* (Plenum Press, 1994).
2. Bender, C. M. & Böttcher, S. Real spectra in non-Hermitian Hamiltonians having *PT* symmetry. *Phys. Rev. Lett.* **80,** 5243–5246 (1998).
3. Bender, C. M., Böttcher, S. & Meisinger, P. N. *PT*-symmetric quantum mechanics. *J. Math. Phys.* **40,** 2201–2229 (1999).
4. Bender, C. M. Must a Hamiltonian be Hermitian? *Am. J. Phys.* **71,** 1095–1102 (2003).
5. Ahmed, Z. Real and complex discrete eigenvalues in an exactly solvable one-dimensional complex *PT*-invariant potential. *Phys. Lett. A* **282,** 343–348 (2001).
6. Levai, G. & Znojil, M. Systematic search for *PT*-symmetric potentials with real spectra. *J. Phys. A* **33,** 7165–7180 (2000).
7. Klaiman, S., Moiseyev, N. & Günther, U. Visualization of branch points in *PT*-symmetric waveguides. *Phys. Rev. Lett.* **101,** 080402 (2008).
8. Bender, C. M., Brody, D. C. & Jones, H. F. Extension of *PT*-symmetric quantum mechanics to quantum field theory with cubic interaction. *Phys. Rev. D* **70,** 025001 (2004).
9. Goldsheid, Y. & Khoruzhenko, B. A. Distribution of eigenvalues in non-Hermitian Anderson models. *Phys. Rev. Lett.* **80,** 2897–2900 (1998).
10. Rotter, I. A non-Hermitian Hamilton operator and the physics of open quantum systems. *J. Phys. A* **42,** 1–51 (2009).
11. Dembowski, C. *et al.* Observation of a chiral state in a microwave cavity. *Phys. Rev. Lett.* **90,** 034101 (2003).
12. El-Ganainy, R., Makris, K. G., Christodoulides, D. N. & Musslimani, Z. H. Theory of coupled optical *PT*-symmetric structures. *Opt. Lett.* **32,** 2632–2634 (2007).
13. Makris, K. G., El-Ganainy, R. & Christodoulides, D. N. Beam dynamics in *PT*-symmetric optical lattices. *Phys. Rev. Lett.* **100,** 103904 (2008).
14. Musslimani, Z. H., El-Ganainy, R., Makris, K. G. & Christodoulides, D. N. Optical solitons in *PT* periodic potentials. *Phys. Rev. Lett.* **100,** 030402 (2008).
15. Mostafazadeh, A. Spectral singularities of complex scattering potentials and infinite reflection and transmission coefficients at real energies. *Phys. Rev. Lett.* **102,** 220402 (2009).
16. Bender, C. M. Making sense of non-Hermitian Hamiltonians. *Rep. Prog. Phys.* **70,** 947–1018 (2007).
17. Znojil, M. *PT*-symmetric square well. *Phys. Lett. A* **285,** 7–10 (2001).
18. Bender, C. M., Brody, D. C., Jones, H. F. & Meister, B. K. Faster than Hermitian quantum mechanics. *Phys. Rev. Lett.* **98,** 040403 (2007).
19. Ahmed, Z. Schrödinger transmission through one-dimensional complex potentials. *Phys. Rev. A* **64,** 042716 (2001).
20. Mostafazadeh, A. Pseudo-Hermiticity versus *PT*-symmetry III: Equivalence of pseudo-Hermiticity and the presence of antilinear symmetries. *J. Math. Phys.* **43,** 3944–3951 (2002).
21. Günther, U. & Samsonov, B. F. Naimark-dilated *PT*-symmetric brachistochrone. *Phys. Rev. Lett.* **101,** 230404 (2008).
22. Bendix, O., Fleischmann, R., Kottos, T. & Shapiro, B. Exponentially fragile *PT* symmetry in lattices with localized eigenmodes. *Phys. Rev. Lett.* **103,** 030402 (2009).
23. Berry, M. Mode degeneracies and the Petermann excess-noise factor for unstable lasers. *J. Mod. Opt.* **50,** 63–81 (2003).
24. Moiseyev, M. & Friedland, S. Association of resonance states with the incomplete spectrum of finite complex-scaled Hamiltonian matrices. *Phys. Rev. A* **22,** 618–624 (1980).
25. Guo, A. *et al.* Observation of *PT*-symmetry breaking in complex optical potentials. *Phys. Rev. Lett.* **103,** 093902 (2009).
26. Kip, D. & Krätzig, E. Anisotropic four-wave mixing in planar $LiNbO_3$ optical waveguides. *Opt. Lett.* **17,** 1563–1565 (1992).
27. Kip, D. Photorefractive waveguides in oxide crystals: Fabrication, properties, and applications. *Appl. Phys. B* **67,** 131–150 (1998).
28. Thylen, L., Wright, E. M., Stegeman, G. I., Seaton, C. T. & Moloney, J. V. Beam-propagation method analysis of a nonlinear directional coupler. *Opt. Lett.* **11,** 739–741 (1986).
29. Tan, Y. *et al.* Formation of reconfigurable optical channel waveguides and beam splitters on top of proton-implanted lithium niobate crystals using spatial dark soliton-like structures. *J. Phys. D* **41,** 102001 (2008).

Acknowledgements

This research was supported by the German–Israeli Foundation for Scientific Research and Development.

Author contributions

C.R. and D.K. performed the experiments at Clausthal. All authors contributed to the theoretical modelling and manuscript preparation.

Additional information

The authors declare no competing financial interests. Reprints and permissions information is available online at http://npg.nature.com/reprintsandpermissions. Correspondence and requests for materials should be addressed to D.K.